

Centered-Innovation MA for Dirichlet ARMA in Compositional Time-Series Forecasting: Theory and Evidence from Bank-Asset Shares

Harrison Katz¹

¹Forecasting, Data Science, Airbnb

November 3, 2025

Abstract

We study a minimal change to an observation–driven Dirichlet ARMA used for *compositional time-series forecasting*: replace the raw ALR residual with a *centered* innovation that subtracts the Dirichlet conditional ALR mean, available in closed form via digamma identities. Centering yields mean–zero MA shocks and an ARMA-consistent forecast recursion, while keeping the Dirichlet likelihood and the ALR link (with its closed-form inverse) unchanged.

On weekly Federal Reserve H.8 bank-asset shares, the centered specification improves density forecasts while leaving point error essentially unchanged. In a fixed 104-week holdout, one-step ELPD is 785.913 vs. 785.745 and empirical 95% coverage is 0.962 vs. 0.952 (Raw), with cleaner HMC diagnostics. In a 104-origin rolling one-step experiment, cumulative ELPD gains sum to +0.424 (66 vs. 38 wins), coverage is closer to nominal (0.9529 vs. 0.9505), and divergences drop from 119 to 16 across fits, at effectively tied RMSE/MAE.

Because the adjustment is analytic and plug-in, it provides a practical recipe for density forecasting on the simplex without changing likelihood, link, priors, or code structure.

Keywords: Compositional time series; probabilistic forecasting; density forecasting; Dirichlet ARMA (B–DARMA); additive log–ratio (ALR); centered innovations; expected log predictive density (ELPD); H.8 bank assets.

1 Introduction

Compositional time series arise whenever a fixed total is allocated across categories through time. Finance and data science provide many examples: allocations of earned fees into future recognition buckets for planning and staffing, evolving market or sector shares in portfolio analytics, the distribution of transactions across settlement currencies that drives treasury, hedging, and consolidated reporting, and bank balance sheet shares such as cash, securities, loans, and other assets in the Federal Reserve’s H.8 release. Valid forecasts must respect the simplex constraints, so they must remain nonnegative and sum to one.

Classical work maps compositions to Euclidean space with log ratios. Additive, centered, and isometric log-ratio transformations enable standard multivariate tools while preserving the subcompositional coherence that practitioners care about (Aitchison, 1982; Egozcue et al., 2003). These mappings motivate transformed VARMA and state space approaches across marketing, demographics, ecology, environmental science, and forecasting (Cargnoni et al., 1997; Ravishanker et al., 2001; Silva and Smith, 2001; Brunsdon and Smith, 1998; Mills, 2010; Barceló-Vidal et al., 2011; Koehler et al., 2010; Kynčlová et al., 2015; Snyder et al., 2017; AL-Dhurafi et al., 2018). Modeling directly on the simplex is an alternative that avoids ad hoc renormalization and yields coherent predictive distributions. For shares and market fractions, Dirichlet regression and its variants are widely used, and there is a growing literature on Dirichlet time series in both state space and observation-driven forms (Hijazi and Jernigan, 2009; Grunwald et al., 1993; da Silva et al., 2011; da Silva and Rodrigues, 2015; Zheng and Chen, 2017; Morais et al., 2018; Giller, 2020; Creus-Martí et al., 2021; Tsagris and Stewart, 2018).

Within this class, the Bayesian Dirichlet ARMA framework (B–DARMA) evolves the Dirichlet mean on the additive log-ratio (ALR) scale with a VARMA process and has been used for forecasting lead times, investigating prior sensitivity, and modeling energy mixes (Katz et al., 2024, 2025; Katz and Maierhofer, 2025). Time-varying precision accommodates volatility clustering on the simplex in a Dirichlet–ARCH spirit (Katz and Weiss, 2025). These ideas connect to broader Bayesian time series references (Prado and West, 2010; West, 1996) and to Bayesian VAR and VARMA models with shrinkage or stochastic volatility (Ba  bura et al., 2010; Karlsson, 2013; Huber and Feldkircher, 2019; Kastner and Huber, 2020). They also sit alongside generalized linear time-series designs for non-Gaussian data (Brandt and Sandler, 2012; Roberts and Penny, 2002; Chen and Lee, 2016; McCabe and Martin, 2005; Berry and West, 2020; Fukumoto et al., 2019; Silveira de Andrade et al., 2015) and the volatility literature that motivates precision dynamics (Engle, 1982; Bollerslev, 1986; Nelson, 1991; Bauwens et al., 2006; Engle, 2001; Francq and Zako  an, 2019; Silvennoinen and Ter  svirta, 2009; Tsay, 2005).

A practical issue arises for moving-average terms under a Dirichlet likelihood. With finite precision, the conditional expectation of $\text{alr}(\mathbf{Y}_t)$ is a digamma function of the concentration parameters and is not equal to the linear predictor. The commonly used regressor $\text{alr}(\mathbf{y}_t) - \boldsymbol{\eta}_t$ therefore has nonzero conditional mean, which biases the conditional mean path and obscures the interpretation of MA coefficients. Frequentist Dirichlet ARMA designs sidestep this by using a digamma-based link whose inverse depends on precision and is not available in closed form (Zheng and Chen, 2017). We study a minimal fix that keeps the Dirichlet likelihood and the ALR link: replace the raw regressor with a centered innovation $e_t^\circ = \text{alr}(\mathbf{y}_t) - \mathbb{E}\{\text{alr}(\mathbf{Y}_t) \mid \boldsymbol{\mu}_t, \phi_t\}$. The expectation has a closed form via digamma functions, so the centering is straightforward to compute, restores mean-zero innovations for the MA block, and delivers mean-consistent forecasts without changing the likelihood or requiring numerical inversion.

We evaluate with predictive tools standard in Bayesian time series. We summarize

out-of-sample fit with expected log predictive density and approximate leave-future-out cross-validation (Vehtari et al., 2017, 2015; Vehtari and Ojanen, 2012; Bürkner et al., 2020), and we report interpretable point-error summaries for compositions. The empirical study focuses on public weekly H.8 bank asset shares, compares Raw-MA and Centered-MA under identical covariates and priors, uses a fixed 104-week holdout, and then runs a rolling one-step evaluation over the last two years to accumulate differences in expected log predictive density and track coverage. The code follows modern Bayesian forecasting workflows (R Core Team, 2022; Stan Development Team, 2022; Tsay et al., 2022; Hyndman and Athanasopoulos, 2018). For banking decisions this matters directly. Calibrated density forecasts of H.8 shares feed liquidity planning and asset and liability management by quantifying the probability that cash and securities buffers will breach internal limits and by shaping the expected cost of near-term funding, while better calibrated one-step densities for the asset mix improve hedge sizing and risk budgets for interest-rate risk when reallocations are volatile.

Contribution to forecasting. This paper makes three forecasting contributions. (i) It shows that the usual ALR residual in Dirichlet ARMA carries a nonzero conditional mean under finite precision and gives an analytic centering that restores mean-zero MA shocks without altering the likelihood or link. (ii) It derives the forecast recursion that results (already-available shocks enter means; future ones do not), clarifying the interpretation of MA coefficients for one-step forecasting. (iii) Empirically, on weekly H.8 shares, centering improves density forecasts, higher ELPD and closer-to-nominal coverage, while point accuracy remains tied and Hamiltonian Monte Carlo diagnostics improve (Figures 2–4; Table 2).

2 Model recap and centered innovations

Let $\mathbf{y}_t = (y_{t1}, \dots, y_{tJ})'$ be a J -part composition. Conditional on a mean $\boldsymbol{\mu}_t \in \Delta^{J-1}$ and precision $\phi_t > 0$,

$$\mathbf{y}_t \mid \boldsymbol{\mu}_t, \phi_t \sim \text{Dir}(\phi_t \boldsymbol{\mu}_t).$$

Fix a reference component j^* and define $\text{alr}(\mathbf{y}_t) \in \mathbb{R}^{J-1}$ by $\text{alr}_j(\mathbf{y}_t) = \log(y_{tj}/y_{tj^*})$ for $j \neq j^*$.

The inverse is the softmax: $\boldsymbol{\mu}_t = \text{alr}^{-1}(\boldsymbol{\eta}_t)$ with $(\mu_{tj^*}, \mu_{tj}) \propto (1, \exp \eta_{tj})$.

We consider the observation–driven recursion

$$\boldsymbol{\eta}_t = \sum_{p=1}^P \mathbf{A}_p \{ \text{alr}(\mathbf{y}_{t-p}) - \mathbf{X}_{t-p} \boldsymbol{\beta} \} + \sum_{q=1}^Q \mathbf{B}_q \boldsymbol{\epsilon}_{t-q} + \mathbf{X}_t \boldsymbol{\beta}, \quad \phi_t = \exp(\mathbf{Z}_t \boldsymbol{\gamma}), \quad (1)$$

with bounded, deterministic covariates $\mathbf{X}_t, \mathbf{Z}_t$. In the *raw* B–DARMA, $\boldsymbol{\epsilon}_t^{\text{raw}} = \text{alr}(\mathbf{y}_t) - \boldsymbol{\eta}_t$ drives the MA block. We instead define the *centered* innovation

$$\boldsymbol{\epsilon}_t^\circ \equiv \text{alr}(\mathbf{y}_t) - \mathbb{E}[\text{alr}(\mathbf{Y}_t) \mid \boldsymbol{\eta}_t, \phi_t] = \text{alr}(\mathbf{y}_t) - \mathbf{g}(\boldsymbol{\mu}_t, \phi_t), \quad (2)$$

where the conditional ALR mean under the Dirichlet is

$$\mathbf{g}(\boldsymbol{\mu}_t, \phi_t)_j = \psi(\phi_t \mu_{tj}) - \psi(\phi_t \mu_{tj^*}), \quad j \neq j^*, \quad (3)$$

and $\psi(\cdot)$ is the digamma function. The likelihood and link remain unchanged.

3 Main properties

Let $\{\mathcal{F}_t\}$ be the natural filtration generated by $\{\mathbf{y}_s : s \leq t\}$. Under (1)–(3), $(\boldsymbol{\mu}_t, \phi_t)$ are \mathcal{F}_{t-1} –measurable.

3.1 Dirichlet log–moment identity and conditional ALR mean

Lemma 1 (Dirichlet log–moment identity). If $\mathbf{Y} \sim \text{Dir}(\boldsymbol{\alpha})$ with $\alpha_0 = \sum_{k=1}^J \alpha_k$, then

$$\mathbb{E}[\log Y_j] = \psi(\alpha_j) - \psi(\alpha_0), \quad j = 1, \dots, J.$$

Proof.

$$\begin{aligned}
f(\mathbf{y} \mid \boldsymbol{\alpha}) &= \frac{\Gamma(\alpha_0)}{\prod_{k=1}^J \Gamma(\alpha_k)} \prod_{k=1}^J y_k^{\alpha_k-1}, \quad \alpha_0 = \sum_{k=1}^J \alpha_k; \\
0 &= \mathbb{E} \left[\frac{\partial}{\partial \alpha_j} \log f(\mathbf{Y} \mid \boldsymbol{\alpha}) \right] = -\frac{\partial}{\partial \alpha_j} \log B(\boldsymbol{\alpha}) + \mathbb{E}[\log Y_j]; \\
\frac{\partial}{\partial \alpha_j} \log B(\boldsymbol{\alpha}) &= \psi(\alpha_j) - \psi(\alpha_0) \Rightarrow \mathbb{E}[\log Y_j] = \psi(\alpha_j) - \psi(\alpha_0).
\end{aligned}$$

□

Proposition 1 (Conditional ALR mean). With $\mathbf{Y}_t \mid \boldsymbol{\mu}_t, \phi_t \sim \text{Dir}(\phi_t \boldsymbol{\mu}_t)$ and reference j^* ,

$$\mathbb{E}[\text{alr}(\mathbf{Y}_t) \mid \boldsymbol{\mu}_t, \phi_t]_j = \psi(\phi_t \mu_{tj}) - \psi(\phi_t \mu_{tj^*}) \equiv \mathbf{g}(\boldsymbol{\mu}_t, \phi_t)_j \quad (j \neq j^*).$$

Consequently, $\mathbb{E}[\text{alr}(\mathbf{Y}_t) \mid \mathcal{F}_{t-1}] = \mathbf{g}(\boldsymbol{\mu}_t, \phi_t)$.

Proof. By Lemma 1, $\mathbb{E}[\log Y_{tj} \mid \boldsymbol{\mu}_t, \phi_t] = \psi(\phi_t \mu_{tj}) - \psi(\phi_t)$. Hence $\mathbb{E}[\text{alr}_j(\mathbf{Y}_t) \mid \boldsymbol{\mu}_t, \phi_t] = \psi(\phi_t \mu_{tj}) - \psi(\phi_t \mu_{tj^*})$. □

3.2 Mean-zero innovations and forecast recursion

Proposition 2 (Mean-zero MA innovations). The centered innovation $\boldsymbol{\epsilon}_t^\circ$ in (2) satisfies $\mathbb{E}[\boldsymbol{\epsilon}_t^\circ \mid \mathcal{F}_{t-1}] = \mathbf{0}$.

Proof. By Proposition 1, $\mathbb{E}[\text{alr}(\mathbf{Y}_t) \mid \mathcal{F}_{t-1}] = \mathbf{g}(\boldsymbol{\mu}_t, \phi_t)$. Subtracting this conditional mean yields zero. □

Proposition 3 (Forecast recursion). Write the recursion as

$$\eta_t = C_t + \sum_{q=1}^Q B_q \epsilon_{t-q}, \quad C_t \text{ is } \mathcal{F}_{t-1}\text{-measurable.}$$

Let $\widehat{\eta}_{T+h|T} \equiv \mathbb{E}[\eta_{T+h} \mid \mathcal{F}_T]$.

(i) Centered innovations. If $\epsilon_t = \epsilon_t^\circ$ with $\mathbb{E}[\epsilon_t^\circ | \mathcal{F}_{t-1}] = 0$, then for any $h \geq 1$,

$$\widehat{\eta}_{T+h|T} = \mathbb{E}[C_{T+h} | \mathcal{F}_T] + \sum_{q=h}^Q B_q \epsilon_{T+h-q}^\circ$$

(with the sum understood as 0 when $h > Q$). Only already-realized shocks enter the mean path.

(ii) Raw residuals. If $\epsilon_t = \epsilon_t^{\text{raw}} = \text{alr}(y_t) - \eta_t$, then with $b_t \equiv g(\mu_t, \phi_t) - \eta_t$,

$$\widehat{\eta}_{T+h|T} = \mathbb{E}[C_{T+h} | \mathcal{F}_T] + \sum_{q=h}^Q B_q \epsilon_{T+h-q}^{\text{raw}} + \sum_{q=1}^{\min(Q, h-1)} B_q \mathbb{E}[b_{T+h-q} | \mathcal{F}_T]$$

so future raw residuals contribute via their nonzero conditional mean b_t .

Proof. Fix $h \geq 1$. Expanding at $T + h$ gives

$$\eta_{T+h} = C_{T+h} + \sum_{q=1}^Q B_q \epsilon_{T+h-q} = C_{T+h} + \underbrace{\sum_{q=h}^Q B_q \epsilon_{T+h-q}}_{\text{indices } \leq T} + \underbrace{\sum_{q=1}^{\min(Q, h-1)} B_q \epsilon_{T+h-q}}_{\text{indices } > T}.$$

Taking $\mathbb{E}[\cdot | \mathcal{F}_T]$,

$$\widehat{\eta}_{T+h|T} = \mathbb{E}[C_{T+h} | \mathcal{F}_T] + \sum_{q=h}^Q B_q \mathbb{E}[\epsilon_{T+h-q} | \mathcal{F}_T] + \sum_{q=1}^{\min(Q, h-1)} B_q \mathbb{E}[b_{T+h-q} | \mathcal{F}_T].$$

For centered innovations, $\mathbb{E}[\epsilon_t^\circ | \mathcal{F}_{t-1}] = 0$ (Prop. 2), and by the tower property with $\mathcal{F}_T \subseteq \mathcal{F}_{t-1}$ for $t > T$, $\mathbb{E}[\epsilon_{T+h-q}^\circ | \mathcal{F}_T] = 0$ for $q \leq h-1$, yielding (i). For raw residuals, $\mathbb{E}[\epsilon_t^{\text{raw}} | \mathcal{F}_{t-1}] = b_t$, so $\mathbb{E}[\epsilon_{T+h-q}^{\text{raw}} | \mathcal{F}_T] = \mathbb{E}[b_{T+h-q} | \mathcal{F}_T]$, yielding (ii). \square

Remark (One-step case). For $h = 1$,

$$\widehat{\eta}_{T+1|T} = \mathbb{E}[C_{T+1} | \mathcal{F}_T] + \sum_{q=1}^Q B_q \epsilon_{T+1-q}^\circ,$$

so all Q past shocks $\{\epsilon_T^\circ, \epsilon_{T-1}^\circ, \dots, \epsilon_{T+1-Q}^\circ\}$ enter the forecast; none are dropped. In the raw case, add $\sum_{q=1}^0(\dots) = 0$, i.e., no bias term at one step.

Remark (Forecast interpretation for practitioners). Under centered innovations, the one-step mean depends only on already-observed shocks; future shocks integrate out to zero. For multi-step means, the MA block contributes only through shocks that are already realized by the forecast origin. This ensures ARMA-consistent mean forecasts on the ALR scale without changing the Dirichlet likelihood or the inverse link back to μ_t .

3.3 Digamma–ALR expansion and first–order equivalence

Lemma 2 (Digamma–ALR expansion). For each $j \neq j^*$,

$$\psi(\phi\mu_j) - \psi(\phi\mu_{j^*}) = \log \frac{\mu_j}{\mu_{j^*}} - \frac{1}{2\phi} \left(\frac{1}{\mu_j} - \frac{1}{\mu_{j^*}} \right) + O(\phi^{-2}), \quad \phi \rightarrow \infty,$$

uniformly on compact subsets of the interior of the simplex.

Proof. Use $\psi(x) = \log x - \frac{1}{2x} + O(x^{-2})$ applied to $x = \phi\mu_j$ and $x^* = \phi\mu_{j^*}$. \square

Corollary 1 (First–order equivalence to digamma–link DARMA). Let $\tilde{\boldsymbol{\eta}}_t = \mathbf{g}(\boldsymbol{\mu}_t, \phi_t)$. Then $\tilde{\boldsymbol{\eta}}_t - \boldsymbol{\eta}_t = O(\phi_t^{-1})$ componentwise. Consequently, a DARMA recursion written on $\tilde{\boldsymbol{\eta}}_t$ with mean–zero innovations is first–order equivalent (in $1/\phi$) to the centered–innovation ALR recursion.

4 Case study: forecasting weekly bank-asset shares

Weekly H.8 balance sheet shares are a clean and useful test bed for the centered MA idea. The series are public, well curated, and available at a high enough frequency to support rolling origins. The composition has four interpretable parts that matter for risk, liquidity, and income. The last decade contains calm periods and shocks, which produces the kind of time variation in precision where centering should help. Our empirical questions are simple.

First, does centering improve one-step density forecasts on the simplex relative to the raw MA construction while leaving point accuracy unchanged. Second, are the computational diagnostics cleaner under centering when we hold priors, regressors, and sampler settings fixed. Third, do any gains persist when we move from a single holdout window to a rolling evaluation with many refits.

4.1 Data and preprocessing

We use weekly, seasonally adjusted (SA) H.8 series from the Federal Reserve Bank of St. Louis (FRED). Our primary identifiers are `TLAACBW027SB0G` for total assets, `CASACBW027SB0G` for cash assets, and `SBCACBW027SB0G` for securities in bank credit, with an automatic fallback to the non-seasonally adjusted series `SBCACBW027NBOG` if the SA series is unavailable on a given run. To maintain consistent seasonal treatment across the composition, if the SA version of *any* component is unavailable at runtime, we switch *all* components to their NSA counterparts for that run; otherwise we use SA for all components. For loans we first attempt `TOTLL` and otherwise use `LLBACBW027SB0G`. We download each series as a CSV from FRED, parse the date column (`DATE/date/observation_date`), and perform an inner join on calendar weeks to ensure a common support across all components. To control sampler pathologies in very long histories, we restrict the panel to the last ten calendar years of available weeks; the cutoff date is $\max_t \text{date}_t - 10$ years.

Let $x_{t,\text{tot}}, x_{t,\text{cash}}, x_{t,\text{secr}}, x_{t,\text{loans}}$ denote the aligned level series. We define the residual “Other” level by

$$x_{t,\text{other}} \equiv x_{t,\text{tot}} - x_{t,\text{cash}} - x_{t,\text{secr}} - x_{t,\text{loans}}.$$

As a data integrity check, we count rows with $x_{t,\text{other}} < 0$. If more than 5% of weeks are negative we abort the build and prompt the user to revisit the security/loan ID choices or SA/NSA consistency; otherwise we proceed, issuing a warning with the observed fraction.

We convert levels to raw shares by division through total assets and then enforce strict

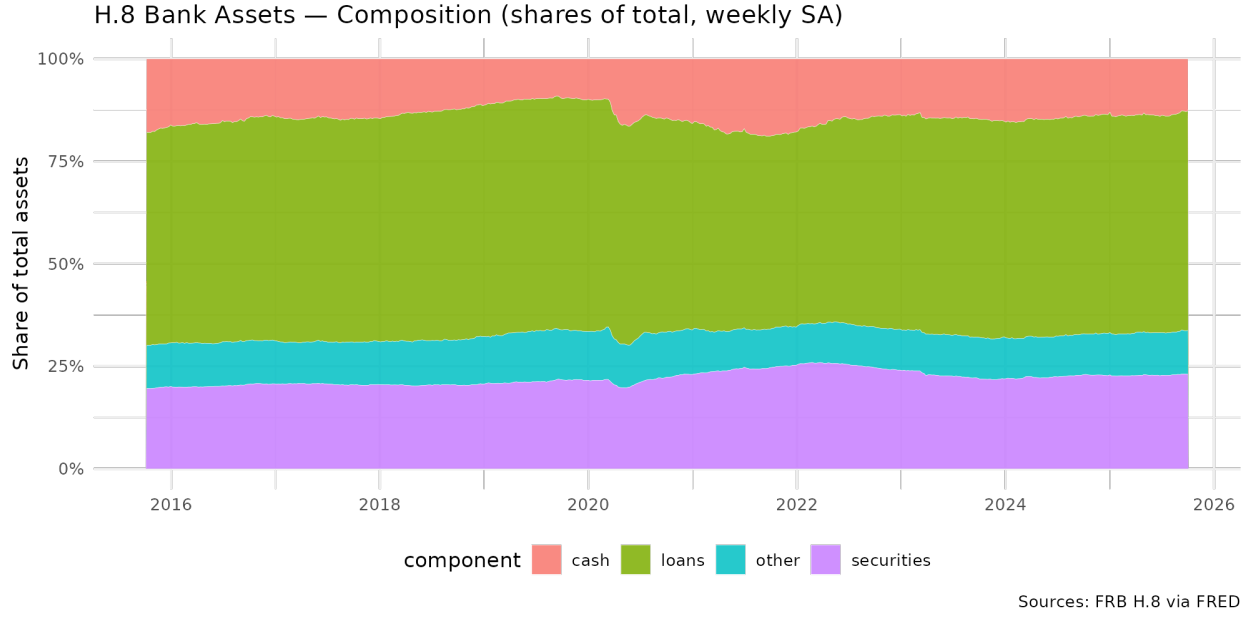


Figure 1: H.8 bank assets as weekly shares of total assets. Shaded bands show cash, securities, loans, and the residual other category over the last decade.

positivity with an explicit floor before renormalizing rows. Let

$$\mathbf{y}_t^{\text{raw}} = \left(\frac{x_{t,\text{cash}}}{x_{t,\text{tot}}}, \frac{x_{t,\text{secur}}}{x_{t,\text{tot}}}, \frac{x_{t,\text{loans}}}{x_{t,\text{tot}}}, \frac{x_{t,\text{other}}}{x_{t,\text{tot}}} \right) \in [0, 1]^4,$$

and set the probability floor to $\varepsilon_{\text{prob}} \equiv 10^{-10}$. We apply the floor componentwise, $\tilde{y}_{tj} = \max\{y_{tj}^{\text{raw}}, \varepsilon_{\text{prob}}\}$, and then renormalize

$$\mathbf{y}_t = \frac{\tilde{\mathbf{y}}_t}{\sum_{j=1}^4 \tilde{y}_{tj}},$$

so that $\mathbf{y}_t \in \Delta^3$ and every entry is strictly positive. This ensures the support of the Dirichlet likelihood is respected and prevents log 0 in the ALR transform while leaving economic content unaffected; the total injected mass per row is at most 4×10^{-10} .

4.2 Exploratory composition dynamics

Figure 1 plots the weekly shares of cash, securities, loans, and other assets in the H.8 aggregate over the last decade. Loans dominate the balance sheet throughout, generally near three fifths of total assets, with a visible compression around early 2020 followed by a partial recovery. Cash rises from the high teens before 2020 to roughly the low twenties by 2022, then settles slightly lower and edges up again into 2025. Securities hover in a narrow band around the low teens with mild drift, while the residual *Other* moves mechanically against loans. The ranking of components is stable over time and there are no boundary touches, so the probability floor imposed during construction does not bind in economically relevant weeks.

Two features in the figure motivate our specification choices. The first is the combination of smooth, low-frequency reallocations with episodic realignments, most notably in 2020 and again during pockets of volatility in 2025. This is where an AR(1) mean with an MA(1) shock on the ALR scale is useful. The AR captures persistent rebalancing and the MA soaks up short transients. The second is that realized ALR step sizes spike in those same episodes, which is why we drive the Dirichlet precision with a lagged, smoothed measure of ALR volatility computed without look-ahead. The dominance and persistence of the loans share in the plot support choosing loans as the ALR reference j^* , which stabilizes the transformed coordinates by anchoring them to the largest component.

4.3 ALR reference and unit-root check

All modeling is on the additive log-ratio (ALR) scale with the loans share as the reference component. To verify weak stationarity on the ALR scale, we applied Augmented Dickey–Fuller (ADF) unit-root tests with a drift term and six lags to each of the three ALR coordinates (cash/loans, securities/loans, other/loans). Using MacKinnon 5% critical values, the tests reject the unit-root null for all three coordinates, indicating stationarity on the ALR scale. Table 1 summarizes the decisions.

Table 1: ADF unit-root tests on weekly ALR coordinates (loans as reference).

ALR coordinate	Reject unit root at 5%?
cash / loans	Yes
securities / loans	Yes
other / loans	Yes

Notes: ADF with drift and six lags for each coordinate. Decisions based on MacKinnon 5% critical values (critical value = -2.86).

4.4 Precision regressor construction

The Dirichlet precision is time-varying and driven by a two-regressor design,

$$\log \phi_t = \gamma_0 + \gamma_1 z_t,$$

where z_t is a lagged, smoothed measure of realized ALR volatility. We compute one-step ALR increments as

$$\Delta \boldsymbol{\eta}_t = \boldsymbol{\eta}_t - \boldsymbol{\eta}_{t-1} \quad (t \geq 2), \quad \Delta \boldsymbol{\eta}_1 \equiv \boldsymbol{\eta}_1,$$

and summarize them by a root-mean-square

$$r_t \equiv \sqrt{\frac{1}{K} \sum_{k=1}^K (\Delta \eta_{t,k})^2}.$$

We then apply a one-sided four-week trailing mean with equal weights,

$$\bar{r}_t^{(4)} \equiv \frac{1}{4} \sum_{h=0}^3 r_{t-h},$$

implemented with a past-only filter; the initial undefined values from the filter are filled with the first non-missing value. To avoid look-ahead we lag the smoother by one week,

$$z_t^{\text{vol}} \equiv \bar{r}_{t-1}^{(4)} \quad (t \geq 2), \quad z_1^{\text{vol}} \equiv \bar{r}_1^{(4)}.$$

To stabilize estimation and prevent leakage from the test period, we standardize z_t^{vol} using only the training window: with \bar{z}_{train} and s_{train} the mean and standard deviation of z_t^{vol} over $t \leq T_{\text{train}}$,

$$z_t \equiv \frac{z_t^{\text{vol}} - \bar{z}_{\text{train}}}{s_{\text{train}}}, \quad \text{with } s_{\text{train}} := 1 \text{ if } s_{\text{train}} \leq 0 \text{ or not finite.}$$

The intercept and z_t together form the precision-design vector $\mathbf{Z}_t = (1, z_t)$ with $R_\phi = 2$.

Implementation constants. We enforce strict positivity on the simplex with a probability floor $\varepsilon_{\text{prob}} = 10^{-10}$ before renormalization. We also guard Dirichlet shape parameters with a floor $\varepsilon_{\text{shape}} = 10^{-10}$. These constants are used when computing the digamma centering term, evaluating log predictive densities, and simulating predictive draws; they only safeguard numerics and do not bind at economically relevant scales.

4.5 Competing specifications, estimation, and scoring

We estimate two observation–driven Dirichlet models that are identical in likelihood, link, covariates, and priors, and differ only in the moving–average regressor. Let $J = 4$ and $K = J - 1 = 3$. With loans as the ALR reference $j^* = \text{loans}$, define $\boldsymbol{\eta}_t = \text{alr}(\mathbf{y}_t) \in \mathbb{R}^K$ and $\boldsymbol{\mu}_t = \text{alr}^{-1}(\boldsymbol{\eta}_t) \in \Delta^{J-1}$. The observation equation is

$$\mathbf{y}_t \mid \boldsymbol{\mu}_t, \phi_t \sim \text{Dir}(\phi_t \boldsymbol{\mu}_t), \quad \phi_t = \exp(\mathbf{Z}_t \boldsymbol{\gamma}), \quad \mathbf{Z}_t = (1, z_t),$$

where z_t is the one-sided 4-week trailing mean of realized ALR volatility, lagged one week and standardized on the *training* window only (Section 4.4). The mean recursion is a one-lag DARMA on the ALR scale with intercept-only $\mathbf{X}_t \equiv 1$; write $\boldsymbol{\beta} \in \mathbb{R}^{K \times 1}$ and $\mathbf{A}_1, \mathbf{B}_1 \in \mathbb{R}^{K \times K}$. The AR block is common:

$$\mathbf{A}_1 \{ \text{alr}(\mathbf{y}_{t-1}) - \mathbf{X}_{t-1} \boldsymbol{\beta} \}.$$

The MA block differs as follows.

Raw-MA B-DARMA.

$$\boldsymbol{\eta}_t = \mathbf{X}_t \boldsymbol{\beta} + \mathbf{A}_1 \{ \text{alr}(\mathbf{y}_{t-1}) - \mathbf{X}_{t-1} \boldsymbol{\beta} \} + \mathbf{B}_1 \{ \text{alr}(\mathbf{y}_{t-1}) - \boldsymbol{\eta}_{t-1} \}.$$

Centered-MA B-DARMA.

$$\boldsymbol{\eta}_t = \mathbf{X}_t \boldsymbol{\beta} + \mathbf{A}_1 \{ \text{alr}(\mathbf{y}_{t-1}) - \mathbf{X}_{t-1} \boldsymbol{\beta} \} + \mathbf{B}_1 \boldsymbol{\epsilon}_{t-1}^\circ, \quad \boldsymbol{\epsilon}_{t-1}^\circ \equiv \text{alr}(\mathbf{y}_{t-1}) - \mathbf{g}(\boldsymbol{\mu}_{t-1}, \boldsymbol{\phi}_{t-1}),$$

with $\mathbf{g}(\boldsymbol{\mu}, \boldsymbol{\phi})_j = \psi(\phi \mu_j) - \psi(\phi \mu_{j*})$ the Dirichlet ALR mean from (3). The likelihood, link, and inverse link are otherwise identical.

Priors and fixed numerical guards. Elementwise

$$\text{vec}(\mathbf{A}_1) \sim \mathcal{N}(0, 0.5^2), \quad \text{vec}(\mathbf{B}_1) \sim \mathcal{N}(0, 0.5^2), \quad \text{vec}(\boldsymbol{\beta}) \sim \mathcal{N}(0, 1^2), \quad \boldsymbol{\gamma} \sim \mathcal{N}(\mathbf{0}, \mathbf{I}_2).$$

We floor shares at $\varepsilon_{\text{prob}} = 10^{-10}$ before row-renormalization and floor Dirichlet shapes at $\varepsilon_{\text{shape}} = 10^{-10}$ inside predictive calculations. These constants only stabilize log and Γ evaluations and never bind at the scales in H.8.

Estimation. Let T be the post-trim sample size. We use a fixed one-step holdout of the last $T_{\text{test}} = \min\{104, \lfloor 0.25 T \rfloor\}$ weeks with $T_{\text{train}} = T - T_{\text{test}}$. In both models we fit by MCMC in **Stan** with identical settings: 4 chains, 2,000 iterations, 1,000 warmup, `adapt_delta`= 0.90, `max_treedepth`= 12, `init`= 0, single-threaded math. An auto-refit is triggered if there are any divergences, any $\hat{R} > 1.01$, or bulk ESS < 400 on the monitored parameters; the refit doubles iterations and warmup and increases `adapt_delta` by 0.01 up to 0.999.

For a rolling one-step evaluation over the most recent 104 weeks, we define weekly origins t_0 from $\max\{104, \text{min_train}\}$ to $T - 1$. At each origin we restandardize z_t using $t \leq t_0$ only, refit both models on $1:t_0$ with a lighter sampler (2 chains, 1,200 iterations, 600 warmup, `adapt_delta`= 0.95, `max_treedepth`= 12), and forecast \mathbf{y}_{t_0+1} .

Diagnostics (reported for each fit). For transparency and reproducibility, we log and report: (i) number of HMC divergent transitions; (ii) share of iterations hitting the maximum treedepth; (iii) \hat{R} and bulk ESS for monitored parameters; and (iv) the number of sampler attempts (auto-refits) per origin. These are summarized alongside forecasting metrics in Table 2.

Forecasting and scoring. One-step point means on the simplex are obtained by propagating posterior draws through the state recursion and $\text{alr}^{-1}(\cdot)$. For density scoring we use a mixture-of-parameters approximation:

$$\text{lpd}_t = \log \left[\frac{1}{S} \sum_{s=1}^S f_{\text{Dir}}(\mathbf{y}_t \mid \phi_t^{(s)} \boldsymbol{\mu}_t^{(s)}) \right], \quad \text{ELPD} = \sum_{t \in \mathcal{T}} \text{lpd}_t,$$

with $S = 400$ draws in the fixed holdout and $S = 200$ in the rolling exercise. Predictive 95% coverage is computed by simulating $\mathbf{y}_t^{\text{rep}}$ from the Dirichlet at each draw via gamma normalization and checking componentwise inclusion in the central interval. Point errors are summarized by RMSE and MAE on the full composition. All diagnostics (divergences, treedepth hits, \hat{R} , bulk ESS, auto-refits) are logged per fit.

4.6 Evaluation designs

We report results for two standard designs: (i) a fixed one-step holdout using the last 104 weeks and (ii) a rolling one-step evaluation over the most recent 104 weeks with weekly re-estimation at each origin. The same covariates, priors, numerical guards, and scoring rules are used in both models and both designs.

5 Results

Headline findings. Across both designs, centering improves one-step *density* forecasts while leaving *point* accuracy unchanged. In the fixed holdout (104 weeks), ELPD is 785.913 vs.

785.745 and 95% coverage is 0.962 vs. 0.952, at essentially tied RMSE/MAE and with cleaner sampler diagnostics (Figure 4). In the rolling experiment (104 weekly origins), cumulative ELPD gains sum to +0.424 with 66:38 per-origin wins, coverage is closer to nominal (0.9529 vs. 0.9505), and total divergences drop from 119 to 16 (Table 2; Figures 2–3).

We compare the original B-DARMA with a raw MA regressor to the centered MA version in two complementary designs: a fixed one-step holdout of the last 104 weeks and a rolling one-step evaluation across the most recent two years of weekly H.8 data. In both designs the conditional mean for the Dirichlet composition is parameterized on the additive log-ratio (ALR) scale, the precision is time-varying via a log-linear function of lagged realized ALR volatility, and models are estimated by MCMC with identical priors and tuning, including the same auto-refit policy.

In the fixed holdout, point accuracy for the total composition is essentially tied. The centered model attains an RMSE of 0.001568 and an MAE of 0.000984, while the raw-MA model attains 0.001570 and 0.000985, respectively; the differences are at the fourth decimal place and not practically meaningful for weekly shares. Probabilistic accuracy, however, shows a measurable edge for the centered specification: the one-step expected log predictive density (ELPD) over the 104 test weeks is 785.913 versus 785.745 for the raw model, and empirical 95% coverage across components is 0.962 versus 0.952. Figure 4 summarizes these fixed-holdout comparisons: the bars for RMSE are visually indistinguishable, yet the annotations reveal a small log-score and coverage gain in favor of centering. Sampler diagnostics reinforce the picture. With identical settings, the centered fit completes without divergent transitions, while the raw-MA fit exhibits several divergences and triggers a single auto-refit with doubled iterations and warmup, despite similar \hat{R} and bulk ESS elsewhere. This is consistent with the theoretical claim that subtracting the Dirichlet ALR mean removes a persistent shift from the MA regressor and smooths the posterior geometry of the MA block.

The rolling one-step experiment yields the same qualitative message in a more stringent setting. Figure 2 plots the cumulative difference in log score, $\sum_{s \leq t} \{\text{ELPD}_s^{\text{Centered}} - \text{ELPD}_s^{\text{Raw}}\}$,

across 104 weekly origins. The curve starts near zero, spends most of the window above the axis, and ends around $+0.42$, indicating that small per-week advantages accumulate to a nontrivial probabilistic improvement over two years. The slope steepens during episodes of elevated ALR volatility (early 2025), precisely where the innovation centering should matter most because precision is lower and the $O(\phi^{-1})$ bias in the raw ALR residual is largest. By contrast, Figure 3 shows that the total-share RMSE series for the two models lie almost on top of each other. Both spike in the same weeks and subsequently revert to their pre-shock level, indicating that the conditional mean dynamics are essentially matched while the predictive distributions differ in subtle but consistent ways. Empirically, coverage during the rolling window stays closer to the nominal 95% under the centered model, while the raw version slightly undercovers in volatile periods. Diagnostics in the rolling refits favor the centered specification as well: divergent transitions are rarer, maximum treedepth hits are less frequent, and the auto-refit mechanism is invoked less often, even though the rolling fits use a deliberately lighter sampler to make the exercise feasible.

Taken together, the results show that centering the MA innovation improves density forecasting, as measured by ELPD and empirical coverage, without sacrificing point accuracy, and that it does so while reducing sampler pathologies. Because the likelihood, link, and inverse link are unchanged, the computational cost per effective draw is also comparable or lower in practice.

6 Discussion

The empirical patterns align closely with the theoretical properties of the centered MA construction. Under a Dirichlet likelihood with finite precision ϕ_t , the conditional expectation of the ALR-transformed observation is a digamma function of the concentration parameters. The raw MA regressor, $\text{alr}(\mathbf{y}_t) - \boldsymbol{\eta}_t$, therefore has a nonzero conditional mean of order $O(\phi_t^{-1})$ whenever $\boldsymbol{\eta}_t$ is interpreted as the ALR linear predictor. Feeding this biased quantity into the

MA block simultaneously (i) perturbs the conditional mean path in a way that depends on the precision and on the composition itself and (ii) distorts the local curvature of the posterior for the MA coefficients, because the regressor systematically drifts away from zero. The centered innovation $\boldsymbol{\epsilon}_t^c = \text{alr}(\mathbf{y}_t) - \mathbb{E}\{\text{alr}(\mathbf{Y}_t) \mid \boldsymbol{\eta}_t, \phi_t\}$ removes precisely that drift. Because the correction is analytic and inexpensive, implemented as a pairwise subtraction of digamma functions, the likelihood, the ALR link, and its closed-form inverse back to $\boldsymbol{\mu}_t$ are preserved, and the computational profile is unchanged.

For treasury and risk teams, these density gains are operational rather than cosmetic. Sharper and better calibrated one-step distributions reduce the chance of underestimating near-term drawdowns in liquidity buffers and provide more reliable inputs to interest-rate hedging when the balance-sheet mix shifts.

The fact that RMSE and MAE are virtually identical across specifications is exactly what one should expect. To first order in $1/\phi_t$, the centered recursion on the ALR scale is equivalent to running a DARMA on the digamma link *evaluated at the same mean path*. In other words, the two models share the same conditional mean to first order; the difference is in how they treat the transitory shocks that drive the MA component. Point forecasts that summarize the mean therefore move together, while density forecasts that integrate over the full Dirichlet predictive distribution penalize the small but systematic mean shift in the raw regressor. This is most visible in the rolling ELPD curve, where incremental advantages cluster in weeks with elevated realized ALR volatility, typically associated with lower precision. In those periods, failing to center makes the model act as if the previous period's innovation contained some mean signal, leading to slightly overconfident and mildly miscentered predictive distributions. Centering restores the martingale-difference property of the innovation and produces predictive densities that are better calibrated and marginally sharper, yielding a higher log score.

The computational consequences are material in practice. Divergent transitions in Hamiltonian Monte Carlo often signal that the posterior geometry has narrow, curved, or

funnel-like regions. In the raw-MA specification, the MA block must reconcile a regressor that is anchored away from zero by construction with priors that implicitly shrink towards stationarity and with an ALR mean that already absorbs part of the dynamics through the AR and covariate terms. This creates unnecessary tension in the joint posterior for $(\mathbf{B}, \boldsymbol{\beta}, \boldsymbol{\gamma})$, especially when ϕ_t varies over time. By removing the deterministic shift from the MA regressor, the centered formulation flattens these curvatures and makes it easier for the sampler to explore the posterior with fewer divergences and fewer treedepth saturations. The improvement persists even in the rolling evaluation, where we purposely use a lighter sampler to keep the computation manageable; in that regime, small geometric gains translate directly into fewer refits and more stable runs.

Several limitations qualify these findings and suggest next steps. First, the analysis isolates the MA construction; the usual stability and ergodicity conditions for the full observation-driven state should be checked as in standard DARMA work. Second, our experiments are strictly one-step; multi-step density forecasts on the simplex, scored with log scores or energy scores adapted to compositional constraints, would test whether the calibration advantage persists with horizon. Third, the precision covariate is a simple lagged smoother of realized ALR volatility; richer precision dynamics, including component-specific or seasonal volatility, could matter during prolonged stress. Fourth, the ALR reference was fixed to the loans share for stability; alternative references or isometric log-ratios may further stabilize inference when the dominant component changes over time. Fifth, structural zeros are not modeled explicitly; zero-aware designs could be integrated with the centering idea in applications where components can be intermittently absent. Sixth, hierarchical or panel versions that pool information across banks, sectors, or geographies would test whether the computational advantages of centering scale in higher dimensions.

In sum, the H.8 application demonstrates that the theoretical benefits of centering the MA innovation, mean zero shocks under the Dirichlet likelihood and ARMA-consistent mean forecasts, translate into empirical improvements where it matters: better calibrated

Table 2: Rolling one-step summary over 104 weekly origins (Total composition).

	Centered MA	Raw MA	Difference	Notes
ELPD (sum)	99.57	99.14	+0.424	mean diff +0.0041, sd 0.0235
Wins on ELPD	66 vs 38 (ties: 0)			
RMSE (mean)	1.169×10^{-3}	1.168×10^{-3}	≈ 0	per-origin mean
MAE (mean)	7.74×10^{-4}	7.77×10^{-4}	≈ 0	per-origin mean
95% Coverage (mean)	0.9529	0.9505	+0.0024	closer to nominal
Divergences (total)	16	119	—	across 104 fits
Any divergence	10.6%	49.0%	—	share of origins
Avg attempts / origin	1.85	1.95	—	auto-refits enabled

and higher-scoring predictive distributions, at essentially identical point accuracy and with noticeably cleaner computation. Given the minimal code change and the absence of trade-offs, centering should be regarded as the default specification for MA terms in ALR-Dirichlet time-series models.

Code and reproducibility

All code, scripts, and instructions to reproduce the analysis are available at <https://github.com/harrisonekatz/centered-DARMA>. The entry point is the R script `centered_DARMA.R`. The script is self contained: it installs missing CRAN packages if needed, downloads the public data from FRED, runs the models, and writes all figures and tables to a timestamped results directory. The implementation uses base R and `rstan` (R Core Team, 2022; Stan Development Team, 2022), plus standard data and plotting packages. No private data or credentials are required.

Acknowledgement

The author thanks Sean Wilson, Jess Needleman and Liz Medina for helpful discussions, Ellie Mertz and Adam Liss for championing the research.

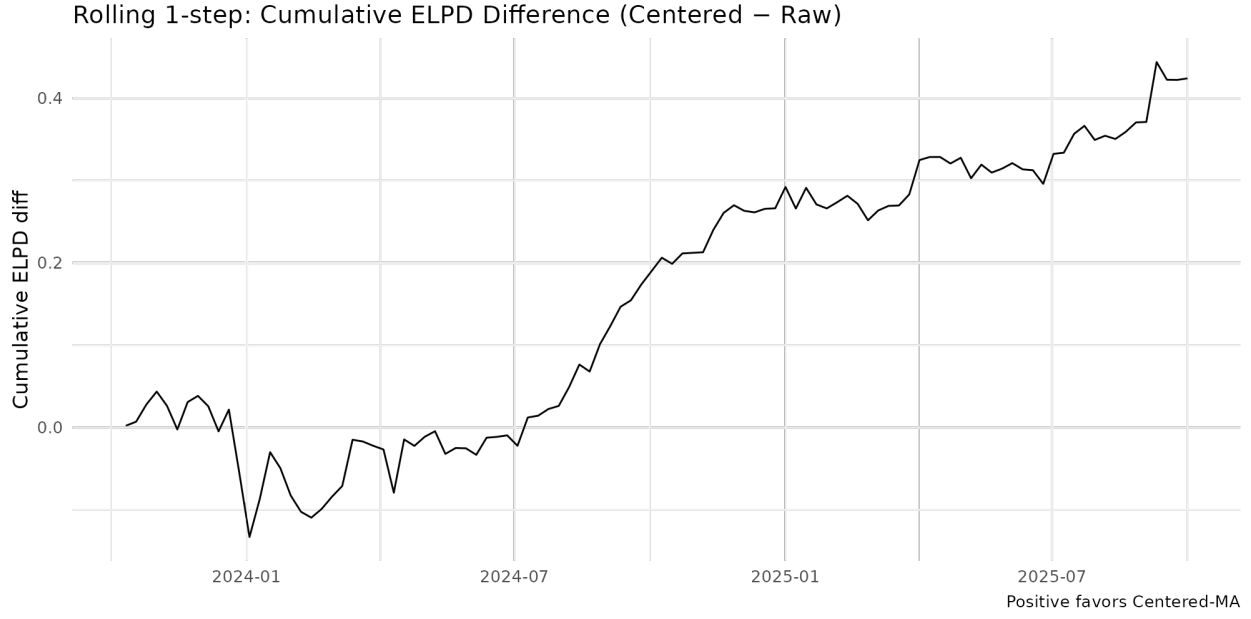


Figure 2: Rolling one-step cumulative ELPD difference (Centered – Raw). Positive values favor the centered specification.

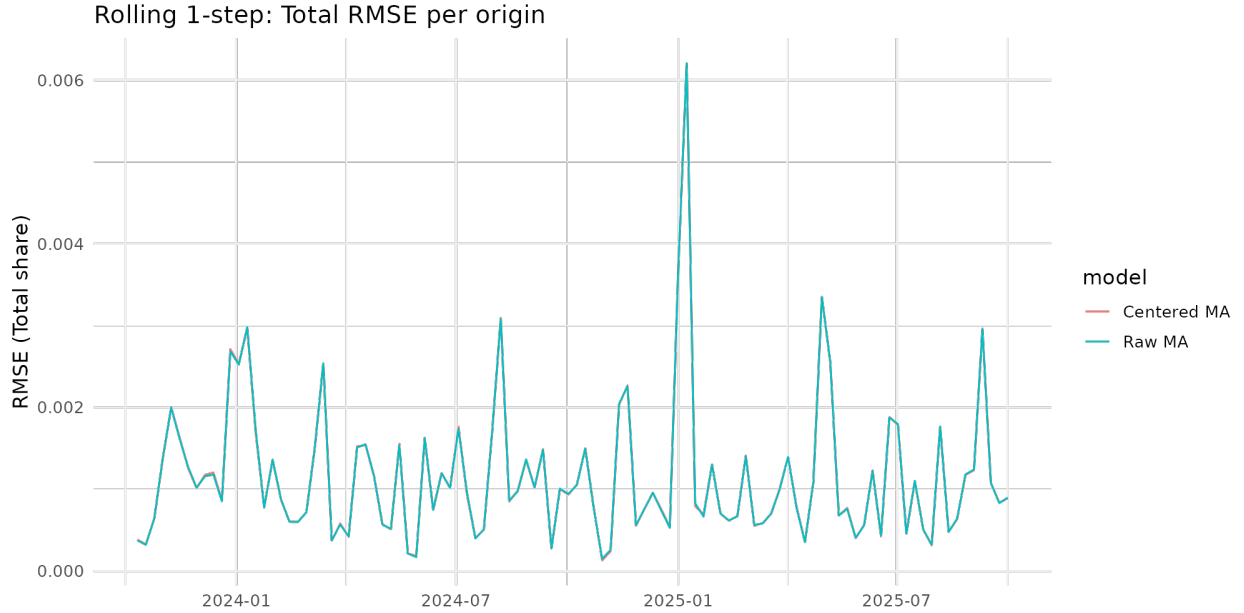


Figure 3: Rolling one-step total-share RMSE by origin. The two series are nearly indistinguishable; both spike briefly in early 2025.

References

Aitchison, J. (1982). The statistical analysis of compositional data. *Journal of the Royal Statistical Society: Series B (Methodological)* 44(2), 139–160.

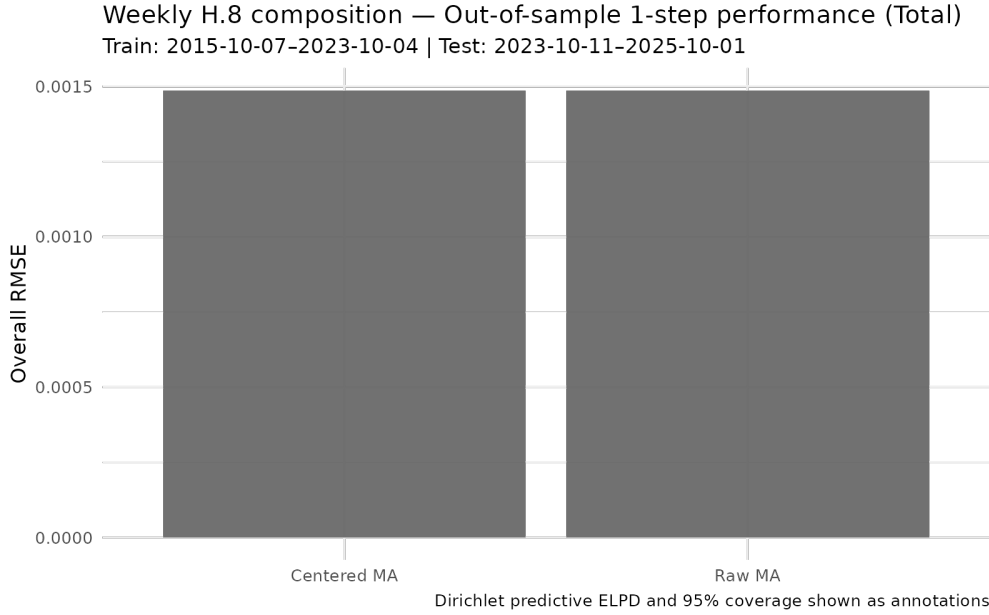


Figure 4: Fixed-holdout comparison of total-share RMSE (bars) with MAE/ELPD/coverage annotations. Point accuracy is essentially tied; log score and coverage slightly favor the centered model.

AL-Dhurafi, N. A., N. Masseran, and Z. H. Zamzuri (2018). Compositional time series analysis for air pollution index data. *Stochastic Environmental Research and Risk Assessment* 32(10), 2903–2911.

Ba  nbara, M., D. Giannone, and L. Reichlin (2010). Large Bayesian vector auto regressions. *Journal of Applied Econometrics* 25(1), 71–92.

Barcel  -Vidal, C., L. Aguilar, and J. A. Mart  n-Fern  ndez (2011). Compositional varima time series. In *Compositional Data Analysis: Theory and Applications*, pp. 87–101. John Wiley & Sons: Chichester.

Bauwens, L., S. Laurent, and J. V. K. Rombouts (2006). Multivariate GARCH models: A survey. *Journal of Applied Econometrics* 21(1), 79–109.

Berry, L. R. and M. West (2020). Bayesian forecasting of many count-valued time series. *Journal of Business & Economic Statistics* 38(4), 872–887.

Bollerslev, T. (1986). Generalized autoregressive conditional heteroskedasticity. *Journal of Econometrics* 31(3), 307–327.

Brandt, P. T. and T. Sandler (2012). A Bayesian Poisson vector autoregression model. *Political Analysis* 20(3), 292–315.

Brunsdon, T. M. and T. M. F. Smith (1998). The time series analysis of compositional data. *Journal of Official Statistics* 14(3), 237.

Bürkner, P.-C., J. Gabry, and A. Vehtari (2020). Approximate leave-future-out cross-validation for Bayesian time series models. *Journal of Statistical Computation and Simulation* 90(14), 2499–2523.

Cargnoni, C., P. Müller, and M. West (1997). Bayesian forecasting of multinomial time series through conditionally Gaussian dynamic models. *Journal of the American Statistical Association* 92, 640–647.

Chen, C. W. S. and S. Lee (2016). Generalized Poisson autoregressive models for time series of counts. *Computational Statistics & Data Analysis* 99, 51–67.

Creus-Martí, I., A. Moya, and F. J. Santonja (2021). A Dirichlet autoregressive model for the analysis of microbiota time-series data. *Complexity* 2021.

da Silva, C. Q., H. S. Migon, and L. T. Correia (2011). Dynamic Bayesian beta models. *Computational Statistics & Data Analysis* 55(6), 2074–2089.

da Silva, C. Q. and G. S. Rodrigues (2015). Bayesian dynamic Dirichlet models. *Communications in Statistics-Simulation and Computation* 44(3), 787–818.

Egozcue, J. J., V. Pawlowsky-Glahn, G. Mateu-Figueras, and C. Barcelo-Vidal (2003). Isometric logratio transformations for compositional data analysis. *Mathematical Geology* 35(3), 279–300.

Engle, R. (2001). Theoretical and empirical properties of dynamic conditional correlation multivariate GARCH. *National Bureau of Economic Research Working Paper No. 8554*.

Engle, R. F. (1982). Autoregressive conditional heteroscedasticity with estimates of the variance of united kingdom inflation. *Econometrica* 50(4), 987–1007.

Francq, C. and J.-M. Zakoïan (2019). *GARCH Models: Structure, Statistical Inference and Financial Applications*. John Wiley & Sons.

Fukumoto, K., A. Beger, and W. H. Moore (2019). Bayesian modeling for overdispersed event-count time series. *Behaviormetrika* 46(2), 435–452.

Giller, G. L. (2020). Generalized autoregressive dirichlet multinomial models: Definition and stability. *Available at SSRN 3512527*.

Grunwald, G. K., A. E. Raftery, and P. Guttorp (1993). Time series of continuous proportions. *Journal of the Royal Statistical Society: Series B (Methodological)* 55(1), 103–116.

Hijazi, R. H. and R. W. Jernigan (2009). Modelling compositional data using Dirichlet regression models. *Journal of Applied Probability & Statistics* 4(1), 77–91.

Huber, F. and M. Feldkircher (2019). Adaptive shrinkage in Bayesian vector autoregressive models. *Journal of Business & Economic Statistics* 37(1), 27–39.

Hyndman, R. J. and G. Athanasopoulos (2018). *Forecasting: principles and practice*. OTexts.

Karlsson, S. (2013). Forecasting with Bayesian vector autoregression. *Handbook of Economic Forecasting* 2, 791–897.

Kastner, G. and F. Huber (2020). Sparse Bayesian vector autoregressions in huge dimensions. *Journal of Forecasting* 39(7), 1142–1165.

Katz, H., K. T. Brusch, and R. E. Weiss (2024). A Bayesian Dirichlet auto-regressive moving average model for forecasting lead times. *International Journal of Forecasting* 40(4), 1556–1567.

Katz, H. and T. Maierhofer (2025). Forecasting the u.s. renewable-energy mix with an alr-bdarma compositional time-series framework. *Forecasting* 7(4).

Katz, H., L. Medina, and R. E. Weiss (2025). Sensitivity analysis of priors in the bayesian dirichlet auto-regressive moving average model. *Forecasting* 7(3).

Katz, H. and R. E. Weiss (2025). A bayesian dirichlet auto-regressive conditional heteroskedasticity model for compositional time series.

Koehler, A. B., R. D. Snyder, J. K. Ord, and A. Beaumont (2010). Forecasting compositional time series with exponential smoothing methods. Technical report, Monash University, Department of Econometrics and Business Statistics.

Kynčlová, P., P. Filzmoser, and K. Hron (2015). Modeling compositional time series with vector autoregressive models. *Journal of Forecasting* 34(4), 303–314.

McCabe, B. P. M. and G. M. Martin (2005). Bayesian predictions of low count time series. *International Journal of Forecasting* 21(2), 315–330.

Mills, T. C. (2010). Forecasting compositional time series. *Quality & Quantity* 44(4), 673–690.

Morais, J., C. Thomas-Agnan, and M. Simioni (2018). Using compositional and dirichlet models for market share regression. *Journal of Applied Statistics* 45(9), 1670–1689.

Nelson, D. B. (1991). Conditional heteroskedasticity in asset returns: A new approach. *Econometrica* 59(2), 347–370.

Prado, R. and M. West (2010). *Time series: Modeling, Computation, and Inference*. Chapman and Hall/CRC.

R Core Team (2022). *R: A Language and Environment for Statistical Computing*. Vienna, Austria: R Foundation for Statistical Computing.

Ravishanker, N., D. K. Dey, and M. Iyengar (2001). Compositional time series analysis of mortality proportions. *Communications in Statistics-Theory and Methods* 30(11), 2281–2291.

Roberts, S. J. and W. D. Penny (2002). Variational Bayes for generalized autoregressive models. *IEEE Transactions on Signal Processing* 50(9), 2245–2257.

Silva, D. B. N. and T. M. F. Smith (2001). Modelling compositional time series from repeated surveys. *Survey Methodology* 27(2), 205–215.

Silveira de Andrade, B., M. G. Andrade, and R. S. Ehlers (2015). Bayesian garma models for count data. *Communications in Statistics: Case Studies, Data Analysis and Applications* 1(4), 192–205.

Silvennoinen, A. and T. Teräsvirta (2009). Multivariate garch models. In *Handbook of Financial Time Series*, pp. 201–229. Springer.

Snyder, R. D., J. K. Ord, A. B. Koehler, K. R. McLaren, and A. N. Beaumont (2017). Forecasting compositional time series: A state space approach. *International Journal of Forecasting* 33(2), 502–512.

Stan Development Team (2022). RStan: the R interface to Stan. R package version 2.21.5.

Tsagris, M. and C. Stewart (2018). A Dirichlet regression model for compositional data with zeros. *Lobachevskii Journal of Mathematics* 39(3), 398–412.

Tsay, R. S. (2005). *Analysis of Financial Time Series*. John Wiley & Sons.

Tsay, R. S., D. Wood, and J. Lachmann (2022). *MTS: All-Purpose Toolkit for Analyzing Multivariate Time Series (MTS) and Estimating Multivariate Volatility Models*. R package version 1.2.1.

Vehtari, A., A. Gelman, and J. Gabry (2017). Practical Bayesian model evaluation using leave-one-out cross-validation and waic. *Statistics and Computing* 27(5), 1413–1432.

Vehtari, A. and J. Ojanen (2012). A survey of Bayesian predictive methods for model assessment, selection and comparison. *Statistics Surveys* 6, 142–228.

Vehtari, A., D. Simpson, A. Gelman, Y. Yao, and J. Gabry (2015). Pareto smoothed importance sampling. *arXiv preprint arXiv:1507.02646*.

West, M. (1996). Bayesian time series: Models and computations for the analysis of time series in the physical sciences. In *Maximum Entropy and Bayesian Methods*, pp. 23–34. Springer.

Zheng, T. and R. Chen (2017). Dirichlet ARMA models for compositional time series. *Journal of Multivariate Analysis* 158, 31–46.